# Synthesis of Platinum Nanoparticles Supported on Poly(acrylic acid) Grafted MWNTs and Their Hydrogenation of Citral

Guiquan Guo,[†] Feng Qin,[‡] Dong Yang,[†] Changchun Wang,*[,†] Hualong Xu,*[,‡] and Shu Yang*[,§]

*Key Laboratory of Molecular Engineering of Polymers and Department of Macromolecular Science and Department of Chemistry, Fudan University, Shanghai 200433, China, and Department of Materials Science and Engineering, University of Pennsylvania, 3231 Walnut Street, Philadelphia, Pennsylvania 19104*

*Received November 13, 2007. Revised Manuscript Received January 10, 2008*

Crystalline Pt nanoparticles were electrolessly deposited on poly(acrylic acid) (PAA) grafted multiwalled carbon nanotubes (MWNTs). The density and uniformity of Pt nanoparticles on MWNTs were found dependent on the PAA grafting density, while their morphologies were tailored by the addition of $NO_3^-$ and $Cu^{2+}$ ions. The catalytic activity and selectivity of hydrogenation of α,β-unsaturated aldehyde, citral, on Pt/MWNTs nanocomposites with different morphologies was studied. The irregularly shaped polycrystalline Pt nanoparticles showed the highest conversion of citral, 92.2%, in comparison to 24.7% from Pt/active carbon, 45.0%, and 40.4% from polyhedrons and polypods Pt single crystals on MWNTs, respectively. The unusually high conversion on Pt/MWNTs suggests a synergistic effect between the PAA grafted MWNTs and the Pt nanoparticles. In the study of the selectivity of hydrogenation, tetra- and octahedron Pt nanoparticles showed the highest ratio of geraniol/nerol, 5.2, ~3 times higher than that of Pt/active carbon, whereas those of irregularly shaped polycrystalline and tetra- and octapods of single crystalline Pt on the MWNTs are 1.9 and 2.2, respectively. Electron diffraction patterns revealed that in the case of tetra- and octahedral Pt particles on the MWNT surface only the {111} facet was exposed, which might induce steric hindrance for the cis-isomers but not for the trans-isomers, whereas the {111} facets were deformed in tetrapods and octapods.

## Introduction

The excellent electronic properties, good physical and chemical stability, and large surface area of carbon nanotubes (CNTs) make them attractive as supporting materials of metal nanoparticles for many potential applications. For example, because of their unique catalytic properties, Pt nanoparticles supported on CNTs are of great interest for selective hydrogenation of α,β-unsaturated aldehydes.[1,2] Although it is known that the catalytic performance (activity and selectivity) of Pt nanoparticles is highly dependent on the structural factors, such as size, morphology and uniformity,[3,4] little has been studied on how the structural factors of Pt nanoparticles supported on CNTs will influence the hydrogenation of α,β-unsaturated aldehydes, such as citral.

To control the nucleation and growth of Pt nanoparticles supported on CNTs, therefore, the structural information of Pt nanoparticles, it will be important to control surface functionality of CNTs and the additives during deposition. Of many functional groups, carboxylic acids are commonly used as nucleation sites for the deposition of metal clusters,[5,6] and can be introduced to CNTs surface through various oxidation methods.[7,8] However, the strong reaction conditions could destroy or shorten CNTs, vary the tubular morphology and their physical properties, or even introduce contaminants, which in turn decreases the activity and selectivity of Pt/CNTs composites. Therefore, it will be desired to develop a nonoxidation approach that covalently grafts carboxylic groups on CNTs with high grafting density and uniformity.

Previously, we have reported a simple yet highly efficient method to covalently graft functional polymers onto single-walled carbon nanotubes (SWNTs) in a poor solvent through a 'fishing' process.[9] It shows promise of synthesizing gram-scale polymer/SWNTs in a small volume of solvent without altering the nanotube electronic properties. Herein, we adapted this method to functionalize multiwalled carbon nanotubes (MWNTs) with poly(acrylic acid) (PAA) with variable degrees for the subsequent electroless deposition of Pt nanoparticles. The density and uniformity of Pt nanopar-

* Corresponding authors. E-mail: ccwang@fudan.edu.cn (C.W.), shuyang@seas.upenn.edu (S.Y.).
[†] Key Laboratory of Molecular Engineering of Polymers and Department of Macromolecular Science, Fudan University.
[‡] Department of Chemistry, Fudan University.
[§] University of Pennsylvania.

(1) Malathi, R.; Viswanath, R. P. *Appl. Catal. A* **2001**, *208*, 323.
(2) Lashdaf, M.; Lahtinen, J.; Lindblad, M.; Venalainen, T.; Krause, A. O. I. *Appl. Catal. A* **2004**, *276*, 129.
(3) Falicov, L. M.; Somorjai, G. A. *Proc. Natl. Acad. Sci. U.S.A.* **1985**, *82*, 2207.
(4) Narayanan, R.; El-Sayed, M. A. *Nano Lett.* **2004**, *4*, 1343.
(5) Hull, R. V.; Li, L.; Xing, Y. C.; Chusuei, C. C. *Chem. Mater.* **2006**, *18*, 1780.
(6) Yu, R. Q.; Chen, L. W.; Liu, Q. P.; Lin, J. Y.; Tan, K. L.; Ng, S. C.; Chan, H. S. O.; Xu, G. Q.; Hor, T. S. A. *Chem. Mater.* **1998**, *10*, 718.
(7) Niyogi, S.; Hamon, M. A.; Hu, H.; Zhao, B.; Bhowmik, P.; Sen, R.; Itkis, M. E.; Haddon, R. C. *Acc. Chem. Res.* **2002**, *35*, 1105.
(8) Tasis, D.; Tagmatarchis, N.; Bianco, A.; Prato, M *Chem. Rev.* **2006**, *106* (3), 1105.
(9) Guo, G. Q.; Yang, D.; Wang, C. C.; Yang, S. *Macromolecules* **2006**, *39*, 9035.

10.1021/cm703225p CCC: $40.75 
Published on Web 02/16/2008

ticles were found dependent on the PAA grafting density, while the crystal morphologies were tailored by the addition of $NO^{3-}$ and $Cu^{2+}$ ions. We then studied the catalytic activity, selectivity to geraniol, and product distribution of hydrogenation of citral using Pt nanoparticles supported on PAA grafted MWNTs with different morphologies.

Citral (3,7-dimethyl-2,6-octadienal) is often chosen as a model compound for selective hydrogenation because it contains both an isolated and a conjugated double bond, as well as a carbonyl group. The products of monohydrogenation of citral, including geraniol, nerol and citronellal, are important in flavoring and perfumery industries.[10] Geraniol, the trans-isomer, is also the major component in insecticides.[11] However, it remains challenging to produce geraniol selectively vs other monohydrogenation products. Ratios of geraniol/nerol of 1.15 and 2 have been reported on Pt/active carbon[12] and Pt/CNTs,[13] respectively. It has been suggested that the morphology of Pt nanoparticles, supports and the presence of functional groups (e.g., -OH and -COOH) are important to improve the selectivity to geraniol. In our experiments, we found that the irregularly shaped polycrystalline Pt on PAA grafted MWNTs (5 wt % Pt loading) possessed the highest catalytic activity (conversion >92%) and a significantly high monohydrogenation selectivity (≈96%) at 60 °C. The high conversion compared to 24.7% from Pt/active carbon clearly indicates the synergistic effect between the MWNTs, PAA and Pt nanoparticles. However, the selectivity to geraniol from irregularly shaped Pt on MWNTs was rather low, 1.9, slightly higher than that of Pt/active carbon, 1.7. When adding $KNO_3$ in Pt precursor solution, $KNO_3/H_2PtCl_6$ = 5.5 mol/mol, tetra- and octahedrons of Pt single crystals were obtained, which exhibited the highest geraniol/nerol ratio, 5.2, among all supported Pt nanoparticles studied in our system. HR-TEM revealed that only {111} facets of the tetra- and octahedral Pt nanoparticles were exposed on MWNTs, which might cause steric hindrance to accommodate the cis-isomers.

## Experimental Section

**Materials.** The MWNTs (purity > 95%, 10∼60 nm diameter, 5−15 $\mu$m length) were synthesized by the chemical vapor deposition (CVD) and purchased from Shenzhen Nanotech Port Co. Ltd. Active carbon (AC, AR, purity > 85%) was purchased from Shanghai Qinghua Chemical Reagent Corporation. 2,2′-Azobisisobutyronitrile (AIBN), acrylic acid (AA), toluene, acetone, ethylene glycol (EG, AR), hexachloroplatinic (IV) acid hexahydrate ($H_2PtCl_6.6H_2O$, AR), $NaNO_3$ and $CuCl_2$, hexane, ethanol and $KBH_4$ were all purchased from Shanghai Chemical Reagent Corporation with purity >95%. Citral ($C_{10}H_{16}O$, purity ≥ 95.0%, a mixture of both E and Z forms (1:1)) was purchased from Sinopharm Chemical Reagent Co. Ltd. Nerol ($C_{10}H_{18}O$, purity ≥ 90%, GC), Geraniol ($C_{10}H_{18}O$, purity ≥ 96%, GC), Citronellol ($C_{10}H_{20}O$, purity 90%∼95%, GC), and Citronellal ($C_{10}H_{18}O$, purity ≥ 80%, GC) were all purchased from Sigma-Aldrich and used as external standard for gas chromatography (GC). AIBN was recrystallized from ethanol. AA was distilled prior to use. All other chemicals were used as received.

**Functionalization of MWNTs with PAA.** In a typical experiment, 1 g acrylic acid (AA) was charged to a three-neck round-bottom reaction flask containing 100 mL acetone and 0.1 g MWNTs. After 10 min sonication (SK3300HP programmable ultrasonic processor, 160 W output with 59 kHz converter), the solution was purged under dry nitrogen for 30 min to remove oxygen, followed by addition of 0.05 g free radical initiator, 2,2′-*azo-bis*-(isobutyronitrile) (AIBN).The reaction was kept at 55 °C for 8 h. The polymer-functionalized MWNTs, PAA-*g*-MWNTs, were carefully washed for five times to remove physically absorbed PAA from MWNTs.

**Deposition of Pt Nanoparticles on MWNTs.** Pt nanoparticles were deposited on the PAA-*g*-MWNTs from the platinum precursor, $H_2PtCl_6$, using ethylene glycol (EG) as solvent and reducing agent. For a typical experiment, the 0.05 g PAA-*g*-MWNTs (PAA grafting amount, 15 wt %) were charged in a 25 mL flask containing 10.0 mL EG and 0.025 g $H_2PtCl_6$. The reaction was carried out at different temperatures depending on the addition of ions. The Pt/MWNTs nanocomposites were then separated from EG solvent by centrifugation (TGL-18C-C, Anting Scientific Instrument Factory, Shanghai), followed by washing for five times. The maximum speed of centrifugation is 18000 rpm, the maximum RCF is 21000*g*, and radial distance is 3 cm. All of the prepared catalysts were dried at 120 °C in oven for 2 h.

**Selective Hydrogenation of Citral.** The hydrogenation of citral was carried out in 100 mL FCZ-1 autoclave with magnetic coupled stirrer at a constant stirring rate (500 rpm). All the catalysts were reduced by $KBH_4$ prior to their use and then preserved in ethanol. 0.5 g of citral was first mixed with 25.0 mL hexane, then 0.05 g (5 wt % Pt loading) catalyst was added to the reactor. Hydrogen was charged into the system to replace the air for three times. The reaction was carried out at 60 °C and 1.0 MPa $H_2$ pressure for 2 h. Reaction products were filtered and analyzed by gas chromatograph (GC).

**Characterization.** Weight loss of PAA-*g*-MWNTs was measured on a TGA instrument (Perkin-Elmer, model Pyris 1 TGA) with platinum pans. The samples were heated from 50 to 800 °C at a heating rate of 10 °C/min under nitrogen (flow rate 20 mL/min). $^1$H NMR analysis was carried out on a Philips DMX500 spectrometer with $D_2O$ as the solvent. High-resolution transmission electron microscopy (HR-TEM) measurements were carried out on a JEM 2010 electron microscope with a field emission source, the accelerating voltage was 200 kV. For the sample preparation, the functionalized MWNTs or Pt/MWNTs composites were dispersed in $H_2O$ for 2 min sonication, then one drop of the solution was placed on a holey copper grid, and the excess of MWNTs suspension was removed. Elemental analysis was performed with an X-ray energy-dispersive spectroscope (EDS) attached to the HRTEM. XPS was performed on a RBD upgraded PHI-5000C ESCA system (Perkin-Elmer) using Al-monochromatic X-ray at a power of 25W with an X-ray-beam diameter of 10 mm, and a pass energy of 29.35 eV. The pressure of analyzer chamber was maintained below $5 \times 10^{-8}$ Pa during the measurement. The binding energy was calibrated using the C 1s photoelectron peak at 284.6 eV as the reference. X-ray diffraction (XRD) analyses were carried out on a PANalytical XMPert powder X-ray diffractometer with Cu Kα radiation, 40 kV, 40 mA). The scan rate, 10 °/min, was applied to record the patterns in the $2\theta$ range of 10°–90°. The reaction products of citral were analyzed by gas chromatography (GC, HP 5890) equipped with a 30m SE-54 capillary column and a flame ionization detector. The injector temperature was 260 °C,

(10) De Simone, R. S.; Gradeff, P. S. U.S. Patent 4,029,709, 1977.
(11) Marin, A. B.; Butler, J. F. U.S. Patent 5,753,686, 1998.
(12) Oksanen, J. A. S.; Mikkola, J. P.; Salmi, T.; Murzin, D. Y. *Catal. Today* **2005**, *102–103*, 128.
(13) Asedegbega-Nieto, E.; Guerrero-Ruiz, A.; Rodrıguez-Ramos, I. *Carbon* **2006**, *44*, 799.

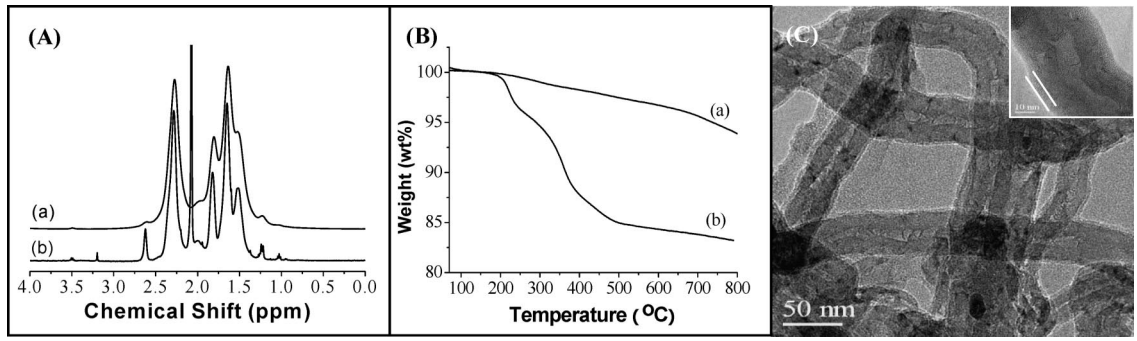


**Figure 1.** Characterization of PAA-*g*-MWNTs: $^1$H NMR spectra of PAA-*g*-MWNTs (A, a) and a mixture of PAA and MWNTs (PAA/MWNTs) (A, b), HRTEM image of PAA-*g*-MWNTs (C, Inset: the white lines indicate the thickness of grafted PAA shell) and TGA curves of pristine MWNTs (B, a) and PAA-*g*-MWNTs (B, b).

and the column temperature was increased from 80 to 260 °C with a ramp rate of 15 °C /min.

## Results and Discussion

**Functionalization of MWNTs with PAA.** The PAA-functionalized MWNTs, PAA-*g*-MWNTs, were synthesized through in situ radical polymerization of AA in its poor solvent, acetone, which was dispersed with MWNTs at 55 °C for 8 h (see details in Experimental Section). The PAA-*g*-MWNTs were then carefully washed for five times to remove physically absorbed PAA from MWNTs. To confirm the existence of covalently grafted polymers on MWNTs, we characterized the PAA-*g*-MWNTs by $^1$H NMR using $D_2O$ as the solvent and compared the chemical shifts of PAA to those that are physically mixed with MWNTs (PAA/MWNTs) (see Figure 1A). While the inherent peaks of PAA, $\delta$ (ppm) = 1.16–2.05 (m, 2H, $CH_2$) and 2.15–2.85 (s, 1H, CH), appeared in both systems, the signals of PAA-*g*-MWNTs were much broader than that of PAA/MWNTs, which could be attributed to slow tumbling of the covalently grafted polymer brushes in solution.[14] HRTEM image of the PAA-*g*-MWNTs clearly showed the polymer shell on the backbone of MWNTs (Figure 1 C), further confirming the successful grafting of PAA on the surface of MWNTs after the *in situ* grafting polymerization. The amount of PAA grafted on MWNTs was estimated as 15 wt % according to TGA measurement (Figure 1 B).

**Deposition of Pt Nanoparticles on MWNTs and Active Carbons (AC).** Several synthetic routes have been proposed to deposit metal nanoparticles onto CNTs, including electrochemical deposition,[15] electroless deposition with or without reducing agents,[16] spontaneous reduction,[17] physical evaporation,[18] and solid state reaction with metal salts at elevated temperatures.[8] Here, electroless deposition was chosen in our system because of its simplicity and mass-producibility. The PAA-*g*-MWNTs (PAA grafting amount, 15 wt %) was mixed with 0.01 M $H_2PtCl_6$ in ethylene glycol (EG) at an elevated temperature for a certain amount of time. A small amount of ions were added to manipulate the crystal morphology of the synthesized Pt nanoparticles. To study the catalytic activity of Pt nanoparticles supported on PAA-*g*-MWNTs, Pt supported on active carbons (Pt/AC) was prepared as reference by impregnating AC with $H_2PtCl_6$ alcohol solutions, followed by reduction under $H_2$ at 300 °C for 30 min.[12]

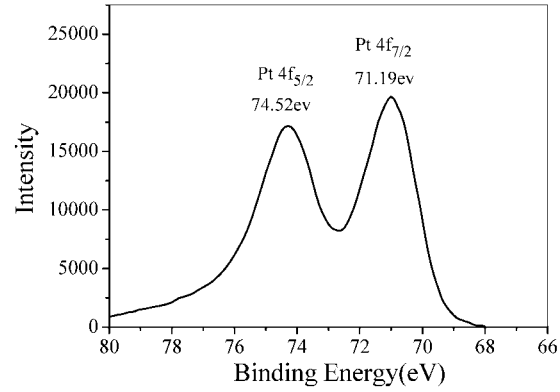


**Figure 2.** XPS spectrum of Pt/PAA-*g*-MWNTs.

The presence of Pt on MWNTs was confirmed by X-ray energy dispersive spectroscopy (EDS, Figure S1, Supporting Information) and X-ray photoelectron spectroscopy (XPS) (Figure 2). As seen in Figure 2, the binding energy of 71.19 and 74.52 eV corresponds to that of Pt $4f_{7/2}$ and Pt $4f_{5/2}$, respectively. Pt nanoparticles deposited on the pristine MWNTs were found randomly dispersed with aggregation (Figure 3A). In contrast, Pt nanoparticles were uniformly deposited on the PAA-*g*-MWNTs (Figure 3B). To further confirm the importance of PAA to the dispersion of Pt nanoparticles on MWNTs, we mixed the pristine and PAA-*g*-MWNTs in 1:1 ratio. As seen in Figure 3C, some MWNTs were loaded with a large amount of well-dispersed Pt nanoparticles (black regions), whereas others almost had none (gray regions, indicated by arrows). These results imply that the -COOH groups on the backbone of PAA served as preferred nucleation sites for reducing metal ions from solution via a coordination reaction or an ion-exchange reaction between Pt precursors and the -COOH. Further evidence can be found in the Supporting Information (Figure S2). The deposited Pt nanoparticles were rather robust and remained on the PAA-*g*-MWNTs after sonication.

(14) Qin, S.; Qin, D.; Ford, W. T.; Resasco, D. E.; Herrera, J. E. *J. Am. Chem. Soc.* **2004**, *126*, 170.
(15) Quinn, B. M.; Dekker, C.; Lemay, S. G. *J. Am. Chem. Soc.* **2005**, *127*, 6146.
(16) Qu, L. T.; Dai, L. M.; Osawa, E. *J. Am. Chem. Soc.* **2006**, *128*, 5523.
(17) Choi, H. C.; Shim, M.; Bangsaruntip, S.; Dai, H. J. *J. Am. Chem. Soc.* **2002**, *124*, 9058.
(18) Kong, J.; Chapline, M.; Dai, H. J. *Adv. Mater.* **2001**, *13*, 1384.

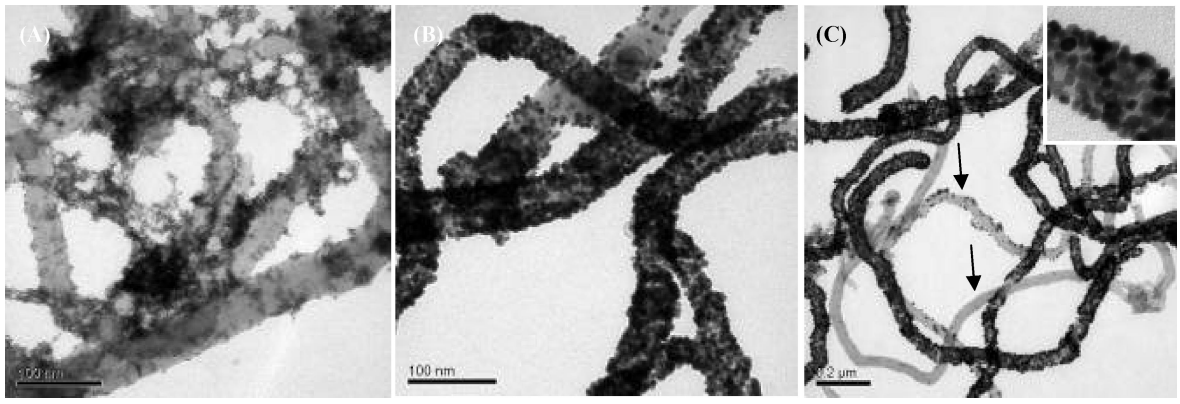


**Figure 3.** HR-TEM images of Pt nanoparticles deposited on different MWNTs: (A) pristine MWNTs, (B) PAA-*g*-MWNTs, and (C) mixture of pristine and PAA-*g*-MWNTs (1:1). PAA grafting amount is 15 wt %. Recipe: 2 mg MWNTs, 1 mg $H_2PtCl_6 \cdot 6H_2O$, and 1 mL EG at 160 °C for 30 min.

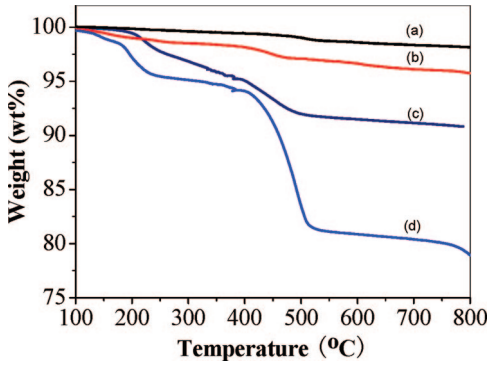


**Figure 4.** TGA curves of (a) Pristine MWNTs, (b) PAA-*g*-MWNTs (centrifugated at 3000 rpm), (c) PAA-*g*-MWNTs (centrifugated between 3000 and 8000 rpm), and (d) PAA-*g*-MWNTs (centrifugated between 8000 and 12000 rpm).

**Effect of PAA Density on the Deposition of Pt Nanoparticles.** The PAA-*g*-MWNTs aqueous solutions were centrifugated at different strength, 3000, 8000, and 12000 rpm, respectively, for 10 min (Figure 4), resulting in different PAA grafting densities, 2, 10 and 22 wt %, respectively. The morphology and size of different PAA-*g*-MWNTs appeared similar (Figure S3, Supporting Information) while the density and uniformity of Pt nanoparticles were clearly improved with the increase of PAA grafting density (Figure 5).

**Size Control of Pt Nanoparticles on PAA-*g*-MWNTs.** The size of Pt nanoparticles plays an important role to the catalytic properties. It can be controlled by preparation conditions, such as reducing agent, temperature and concentration of Pt precursors. The stronger the reducing agent, the higher the reducing rate, and the smaller the metal nanoparticles. When $NaBH_4$, a stronger reducing agent than HCHO, was used, more Pt nuclei were produced in a short period of time, resulting in smaller Pt nanoparticles on PAA-*g*-MWNTs (Figure 6A) compared to those reduced by HCHO (Figure 6B). Temperature could also influence the crystal nucleation and growth. Using EG as reducing agent, more Pt nuclei were produced with smaller Pt nanopartciles at 160 °C (Figure 6C) than those at 140 °C (Figure 6D).

In the study of the effect of concentration of Pt precursors, PAA-*g*-MWNTs (2 mg) and $H_2PtCl_6 \cdot 6H_2O$ (1 mg) were dispersed in various amounts of EG, 1, 5, and 10 mL, respectively, at 160 °C for 30 min. The synthesized Pt/MWNTs nanocomposites were characterized by HR-TEM and XRD (Figure 7). The diffraction peaks in XRD at $2\theta =$ 26.5°, 42.4°, 54.7° and 77.4° (Figure 7D) were assigned to (002), (100), (004) and (110) planes, respectively, of the hexagonal graphite structures of PAA-*g*-MWNTs. The crystal structure of Pt nanoparticles was confirmed as face centered cubic (fcc) given the presence of diffraction peaks at $2\theta =$ 39.7°, 46.2°, 67.4°, 81.2° and 85.4°, corresponding to (111), (200), (220), (311), and (222) planes, respectively.[19] The average size of Pt particles increased with the concentration of Pt precursors from ~1.3 nm ($H_2PtCl_6 \cdot 6H_2O$/EG = 0.1 mg/mL), 3.2 nm (0.2 mg/mL) to 8.7 nm (1 mg/mL), as

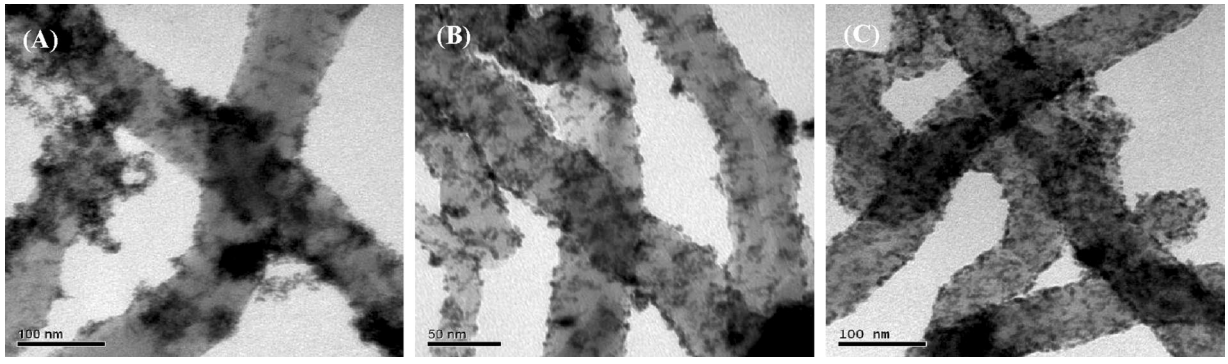


**Figure 5.** HR-TEM images of the deposited Pt nanoparticles on the surface of PAA-*g*-MWNTs centrifugated out at different strengths: (A) 3000 rpm, (B) between 3000 and 8000 rpm, and (C) between 8000 and 12000 rpm. Pt deposition recipe: 20 mg MWNTs, 0.5 mg $H_2PtCl_6 \cdot 6H_2O$, 10 mL EG at 160 °C for 30 min.

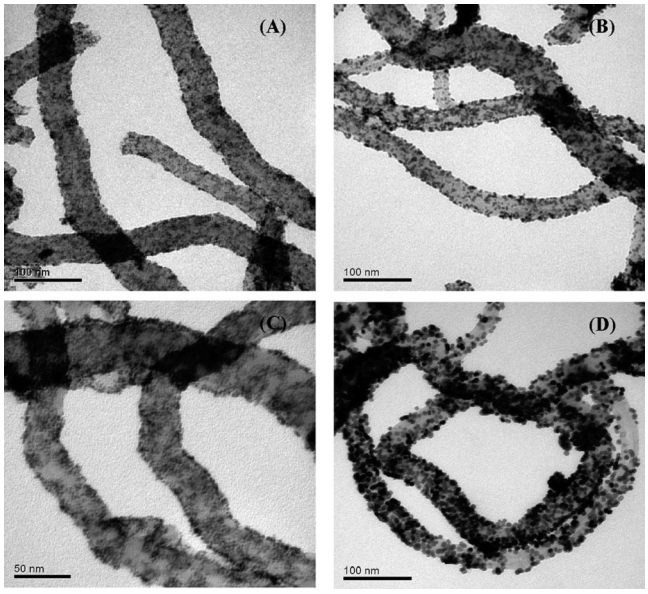


**Figure 6.** HR-TEM images of Pt/MWNTs nanocomposites synthesized with different reducing agents: (A) $NaBH_4$ at room temperature, (B) HCHO at room temperature, (C) EG at 160 °C, and (D) EG at 140 °C.

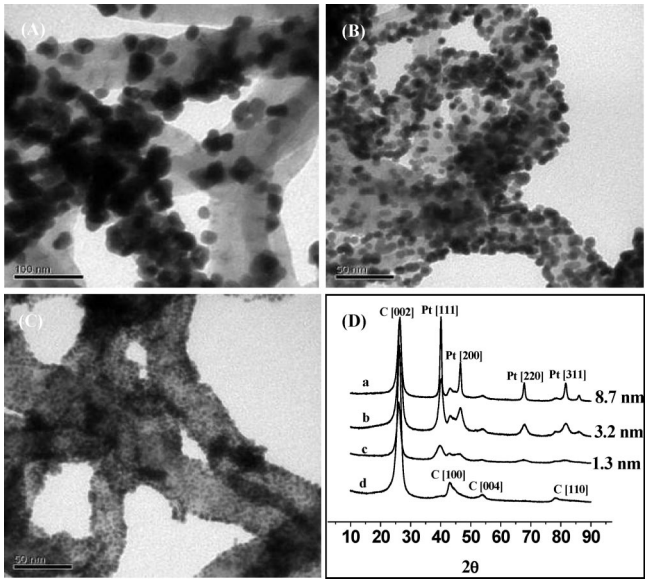


**Figure 7.** (A−C) HR-TEM images of Pt/MWNTs nanocomposites prepared from different $H_2PtCl_6 \cdot 6H_2O$/EG ratios: (A) 1 mg/mL, (B) 0.2 mg/mL, and (C) 0.1 mg/mL at 160 °C for 30 min. (D) XRD of (a−c) Pt deposited on MWNTs shown in (A−C) and (d) bare PAA-*g*-MWNTs.

determined by Sherrer's formula through line broadening of the Pt (220) peak.[20]

**Morphology Control of Pt Nanoparticles.** In addition to particle size, morphology of metal nanoparticles could play a critical role in tailoring the electronic, optical, magnetic, and catalytic properties of inorganic nanoparticles.[21,22] It has been shown that a small amount of ion additives could influence the morphology and crystal structures of Pt nanoparticles.[16,23] To follow the morphological evolution of Pt nanoparticles grown on PAA-*g*-MWNTs, we systematically varied the molar ratios of $KNO_3/H_2PtCl_6$ in solutions. In the absence of $KNO_3$, Pt nanoparticles appeared irregular with size ranging from 5 to 7 nm (Figure 8A). Addition of $KNO_3$ led to the formation of larger single crystals of Pt nanoparticles, and the crystal shape changed from tetra- and octahedral (Figure 8B) to tetra- and octapods (Figure 8C) when the molar ratio of $KNO_3/H_2PtCl_6$ was increased from 5.5 to 11. The results are in good agreement with the observation of Pt nanoparticles synthesized in solution.[23] The size of the single crystalline Pt nanoparticles appeared larger than that of the irregular polycrystalline ones, while the density of the latter on the surface of PAA-*g*-MWNTs was higher (Figures 8B and 8C). When replacing $KNO_3$ with $CuCl_2$, Pt nanocubes were obtained on the surface of MWNTs at 110 °C for 18 h (Figure 8D), similar to that from aqueous solution.[16]

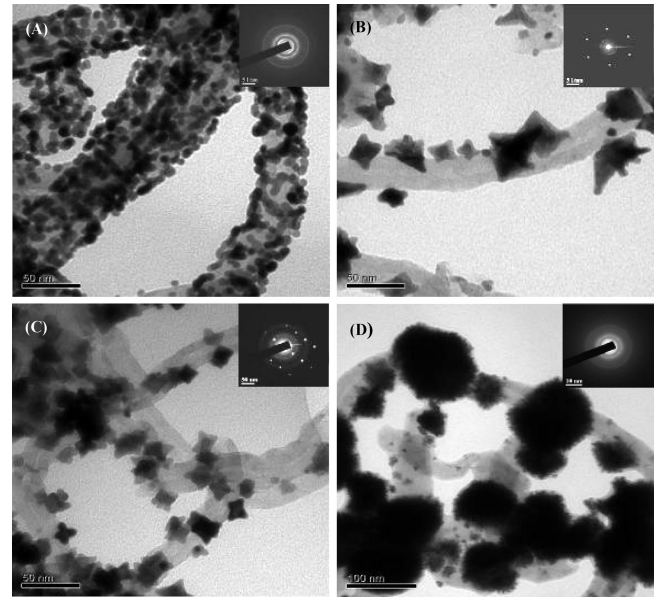


**Figure 8.** HR-TEM images of Pt nanoparticles supported on PAA grafted MWNTs in the presence of different additives. (A) No $KNO_3$, (B) $nKNO_3$: $nH_2PtCl_6 = 5.5$, (C) $nKNO_3$:$nH_2PtCl_6 = 11$, and (D) $CuCl_2$, 10 mg/mL. Insets: electronic diffraction patterns. (B) Viewed from [111] direction and (C) viewed from [110] direction. Pt deposition recipe: 50 mg MWNTs, 25 mg $H_2PtCl_6 \cdot 6H_2O$ and 10 mL EG at 160 °C, 30 min (A−C) and at 110 °C, 18 h (D). The scale bars are 50 nm in A−C and 100 nm in D, respectively.

The catalytic performance of Pt nanoparticles is known highly dependent on the exact arrangement between atoms on the exposed facets.[3] Therefore, it will be highly desired to synthesize monodispersed, uniformly faceted particles for high specificity in a catalytic process. Electronic diffraction of TEM images showed that the irregularly shaped Pt nanoparticles and Pt nanocubes supported on MWNTs were polycrystalline (inset in Figure 8A,D), whereas the tetra-, octahedral (Figure 8B) and tetra-, octapods (Figure 8C) Pt nanoparticles were fcc single crystals. It is worth noting that the tetra-, octahedral Pt crystals are all bounded by {111} facets (Figure 8B inset), which, on the other hand, are

(19) Fujiwara, N.; Yasuda, K.; Ioroi, T.; Siroma, Z.; Miyazaki, Y. *Electrochim. Acta* **2002**, *47*, 4079.
(20) Radmilovic, V.; Gasteiger, H. A.; Ross, P. N. *J. Catal.* **1995**, *154*, 98.
(21) Chen, S.; Wang, Z. L.; Ballato, J.; Foulger, S.; Carroll, D. *J. Am. Chem. Soc.* **2003**, *125*, 16186.
(22) Sau, T. K.; Murphy, C. J. *J. Am. Chem. Soc.* **2004**, *126*, 8648.
(23) Herricks, T.; Chen, J. G.; Xia, Y. N. *Nano Lett.* **2004**, *4*, 2367.

**Scheme 1. Illustration of the Possible Reactions in Hydrogenation of Citral**

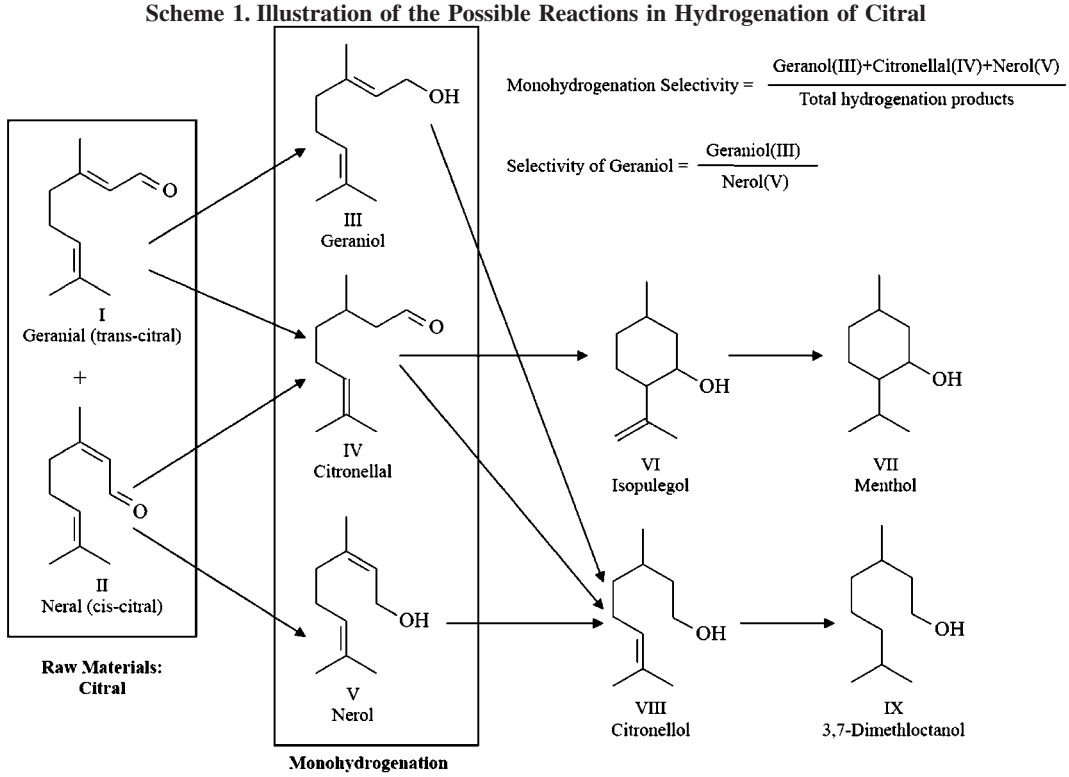


**Table 1. Catalytic Results of Citral (I+II) Hydrogenation over a Series of Pt/MWNTs and Pt/AC Catalysts[a]**

| | | product distribution (wt %) | | | | | |
|---|---|---|---|---|---|---|---|
| catalyst | conversion (%) | III | IV | V | others | monohydrogenation selectivity (%) | selectivity to geraniol |
| Pt/AC | 24.7 | 12.0 | 73.8 | 7.2 | 7.0 | 93.0 | 1.7 |
| Pt/MWNTs-1 (irregular) | 92.2 | 5.8 | 87.1 | 3.0 | 4.1 | 95.9 | 1.9 |
| Pt/MWNTs-2 (tetra-, octahedral) | 45.0 | 10.8 | 53.6 | 2.1 | 33.5 | 66.5 | 5.2 |
| Pt/MWNTs-3 (tetra-, octapods) | 40.4 | 21.3 | 12.4 | 9.8 | 56.6 | 43.4 | 2.2 |

[a] Reaction conditions: $T = 60$ °C; $P(H_2) = 1.0$ MPa; $m_{Pt}/m_{CNT} = 0.05$ g; $m_{citral} = 0.5$ g; $V_{hexane} = 25$ mL; rotate speed = 500 rpm, and reaction for 2 h. Pt nanoparticles loading is 5 wt %.

deformed in octapods and tetrapods crystals (Figure 8C inset). It has been suggested that the Pt crystals grow mainly along the [100] directions for tetrapods and the [111] directions for octapods in the high ratio of $KNO_3/H_2PtCl_6$.[23] In the following section, we demonstrate that the morphologies of single crystal Pt nanoparticles supported on MWNTs play critical roles in catalytic hydrogenation of citral in terms of conversion and selectivity.

**Selective Hydrogenation of Citral.** The evolution of selective hydrogenation of citral is shown in scheme 1.[12,13] The ratio of monohydrogenation products (geraniol, nerol and citronellal) to the overall hydrogenation products is defined as monohydrogenation selectivity (MS). The ratio of monohydrogenation isomer products, geraniol/nerol, is defined as selectivity to geraniol.

The activity, monohydrogenation selectivity and selectivity to geraniol of Pt catalysts on different supports, Pt/AC and Pt/MWNTs, for hydrogenation of citral were evaluated according to the distribution of products (Figure S4, Supporting Information). In our experiments, the conversion of citral from the irregularly shaped Pt/MWNTs (Pt/MWNTs-1) was unusually high, 92.2%, compared to that of 24.7% from Pt/AC (see Table 1), and citronellal was the main product from both Pt nanocomposites. The high conversion on Pt/MWNTs may be attributed to (1) the good dispersibility of Pt nanaoparticles and (2) characteristics of MWNTs as catalyst–support for good hydrogen adsorption, fast diffusion and transport properties.[24,25] Pt/MWNTs-1 showed the highest monohydrogenation selectivity, 95.9%, in combination of a high conversion (92.2%), among all the Pt/MWNTs, which will be especially attractive for mass production. For the polyhedrons and polypods of Pt nanoparticles supported on MWNTs, the conversion was 45.0% and 40.4%, respectively, and the products other than monohydrogenation increased substantially. In the case of polypods (Pt/MWNTs-3), citronellal became the minor product (see Table 1). In addition, the latter two single crystal Pt nanoparticles showed lower monohydrogenation selectivity, 66.5% and 43.4%, respectively. It has been suggested that hydrogenation activity increases with the surface roughness of the Pt nanoparticles.[26]

On the irregular polycrystalline Pt nanoparticles, many facets were exposed, thus, it was not surprising that they showed the highest conversion and selectivity in monohy-

(24) Miyamoto, J.; Hattori, Y.; Noguchi, D.; Tanaka, H.; Ohba, T.; Utsumi, S.; Kanoh, H.; Kim, Y. A.; Muramatsu, H.; Hayashi, T.; Endo, M.; Kaneko, K. *J. Am. Chem. Soc.* **2006**, *128*, 12636.
(25) Holt, J. K.; Park, H. G.; Wang, Y. M.; Stadermann, M.; Artyukhin, A. B.; Grigoropoulos, C. P.; Noy, A.; Bakajin, O. *Science* **2006**, *312*, 1034.
(26) Birchem, T.; Pradier, C. M.; Berthier, Y.; Cordiery, G. *J. Catal.* **1996**, *161*, 68.

drogenation, while possessing very low selectivity to geraniol, geraniol/nerol = 1.9, close to the feeding ratio of geranial/neral, 1.1. In contrast, on tetra-, octahedral Pt nanoparticles (Pt/MWNTs-2) the highest geraniol/nerol ratio, 5.2, was obtained, approximately three times higher than that of Pt/AC (Table 1). The high selectivity to geraniol may be attributed to the close-packed structure and the steric hindrance in tetra-, octahedral Pt single crystals, where only the {111} facet is exposed; it is difficult for Pt nanoparticles to accommodate the cis-isomer (nerol) but not for the *trans*-isomer (geraniol).[26] We note that this result is different from the previously reported steric constraints for the *trans*-isomers but not for the *cis*-isomers on Pt/AC[12] and Pt/CNTs.[13] Although the Pt polypods were also single crystals, their selectivity to geraniol was found low (2.2). The electron diffraction (Figure 8C inset) showed a deformed {111} facet, which might result in less steric hindrance for nonselective hydrogenation. We found that when depositing Pt nanoparticles from high ratios of $KNO_3/H_2PtCl_6$, the nanoparticles grew faster at areas with high curvatures, i.e, corners and edges, than that of the centers where the {111} facet was deformed. Similar findings were reported in the growth of Pt nanoparticles in solution.[23] Currently, we are optimizing the Pt nanoparticle deposition reactions to tailor the crystal morphology, size and uniformity so that we can achieve both high yield and high selectivity of geraniol production.

## Conclusion

In summary, we have synthesized PAA-grafted MWNTs by in situ polymerization of PAA in its poor solvent for deposition of Pt nanoparticles. The PAA grafting density was controlled by varying the reaction conditions and strength of centrifugation, which in turn determined the density and uniformity of Pt nanoparticles deposited on MWNTs. With the increase of the concentration of Pt precursors, the size of Pt nanoparticles increased along with decrease of the particle density. The Pt nanoparticle morphologies were altered by addition of ions during the deposition process to study their effect on catalysis on hydrogenation of citral. Irregular, polyhedrons, polypods Pt nanoparticles were loaded on MWNTs in the presence of different molar ratios of $KNO_3/H_2PtCl_6$, whereas Pt nanocubes were obtained with addition of a small amount of $Cu^{2+}$. The irregularly shaped Pt polycrystals showed the highest catalytic activity, monohydrogenation selectivity, implying a synergistic effect between the support of MWNTs and the Pt nanoparticles. The irregularly shaped Pt polycrystals exhibited the highest activity and monohydrogenation selectivity in all systems studied here. In contrast, the polyhedral single crystal Pt nanoparticles bounded by {111} facets showed the highest selectivity to geraniol, which might be due to steric hindrance induced by the close-packed structure of {111} facets for the cis-isomers but not for the trans-isomers of citral. We believe that the controlled synthesis of Pt nanoparticles on polymer grafted MWNTs and study of their catalytic effect dependence on Pt structural factors offer important insights to achieve both high catalytic activity and selectivity of Pt/CNTs nanocomposites.

**Acknowledgment.** This work was supported by National Science Foundation of China (Grants 20728404 and 20674009), the National Science Foundation for Distinguished Young Scholars of China (50525310), the Cultivation Fund of the Key Scientific and Technical Innovation Project, Ministry of Education of China (707023), and Shanghai Leading Academic Discipline Project (B113). S.Y. would like to acknowledge the MRSEC Program of the National Science Foundation under Award No. DMR05-20020 and the Advanced Scholars Program of Fudan University.

**Supporting Information Available:** Additional figures and details including EDS of Pt/PAA-*g*-MWNTs, HRTEM images of PAA-*g*-MWNTs, SEM images of MWNTs, and GC characterization of citral hydrogenation products. This material is available free of charge via the Internet at http://pubs.acs.org.

CM703225P